ARTICLES
https://doi.org/10.1038/s41559-022-01693-3
nature ecology & evolution

Check for updates

Extinction, coextinction and colonization dynamics in plant–hummingbird networks under climate change

Jesper Sonne[1,2]✉, Pietro K. Maruyama[3], Ana M. Martín González[4], Carsten Rahbek[1,2,5,6], Jordi Bascompte[7] and Bo Dalsgaard[1]

Climate-driven range shifts may cause local extinctions, while the accompanying loss of biotic interactions may trigger secondary coextinctions. At the same time, climate change may facilitate colonizations from regional source pools, balancing out local species loss. At present, how these extinction–coextinction–colonization dynamics affect biological communities under climate change is poorly understood. Using 84 communities of interacting plants and hummingbirds, we simulated patterns in climate-driven extinctions, coextinctions and colonizations under future climate change scenarios. Our simulations showed clear geographic discrepancies in the communities' vulnerability to climate change. Andean communities were the least affected by future climate change, as they experienced few climate-driven extinctions and coextinctions while having the highest colonization potential. In North America and lowland South America, communities had many climate-driven extinctions and few colonization events. Meanwhile, the pattern of coextinction was highly dependent on the configuration of networks formed by interacting hummingbirds and plants. Notably, North American communities experienced proportionally fewer coextinctions than other regions because climate-driven extinctions here primarily affected species with peripheral network roles. Moreover, coextinctions generally decreased in communities where species have few overlapping interactions, that is, communities with more complementary specialized and modular networks. Together, these results highlight that we should not expect colonizations to adequately balance out local extinctions in the most vulnerable ecoregions.

Biotic interactions are the glue that connects species within ecological communities[1–3]. When climate change forces a species to emigrate from a local community, the remaining species may lose fitness due to the accompanying loss of biotic interactions[4–7]. Particularly in communities consisting of mutualistic dependent species, such as plants and animal pollinators, the loss of biotic interactions could ultimately cause local secondary extinctions[8,9]. Thereby, climate-induced range shifts in individual species could have cascading impacts on the entire community[10–13].

Several studies have simulated disruptions of plant–pollinator interaction networks with theoretical expectations for how secondary extinctions could spread between species[14–17]. Recent examples further combined network simulations with climate niche models to investigate local extinctions under future climate change[8,9]. These studies differentiated between species loss as a direct consequence of climate change (climate-driven extinctions) and species loss due to the extinction of their mutualistic partners (coextinctions). By combining these two extinction processes, mutualistic communities become more vulnerable to climate change than anticipated when only considering climate-driven extinctions[9]. Nevertheless, these simulations ignored that communities may also gain new species by colonization as they track climate change[18]. If such colonization events balance out local extinctions, mutualistic communities could maintain their structural integrity. Thus, ignoring colonizations from regional source pools may overestimate the detrimental effect of climate change on ecological communities.

Here, we use future climate scenarios to simulate climate-driven extinction, coextinction and colonization processes in 84 plant–hummingbird pollination networks sampled across the American mainland. Plant–hummingbird interactions constitute an ideal model system because our analytical framework requires high-resolution occurrence data and biotic interactions sampled across a large geographical extent. The plant–hummingbird system meets both of these criteria as the hummingbird's geographic distributions are well known[19,20] and their interactions with plants were recently supported by a comprehensive database[21]. Our simulations run in a four-step procedure. First, we combined geographical presence–absence data with altitudinal range limits to predict the hummingbirds' distributions onto a digital terrain model (Fig. 1a). From these distributions, we extracted four contemporary climate variables and used them to determine each species' occupied climate volume.

In the second stage, we calculate the climate-driven extinction rate for a given hummingbird species i in a focal community j (Fig. 1b). Here, we calculate the standardized distance (z-score) from the centroid of a species' climate volume to current and future climate conditions in the community—d_{ij} and d'_{ij}, respectively. Using these z-scores, we calculate the proportion of the ith species' climate volume that takes values within ($d'_{ij} - d_{ij}$) and d'_{ij}

[1]Center for Macroecology, Evolution and Climate, GLOBE Institute, University of Copenhagen, Copenhagen, Denmark. [2]Center for Global Mountain Biodiversity, GLOBE Institute, University of Copenhagen, Copenhagen, Denmark. [3]Centre for Ecological Synthesis and Conservation, Department of Genetics, Ecology and Evolution—ICB, Federal University of Minas Gerais (UFMG), Belo Horizonte, Brazil. [4]Pacific Ecoinformatics and Computational Ecology Lab, Berkeley, CA, USA. [5]Institute of Ecology, Peking University, Beijing, China. [6]Danish Institute for Advanced Study, University of Southern Denmark, Odense, Denmark. [7]Department of Evolutionary Biology and Environmental Studies, University of Zurich, Zurich, Switzerland. ✉e-mail: jesper.sonne@sund.ku.dk

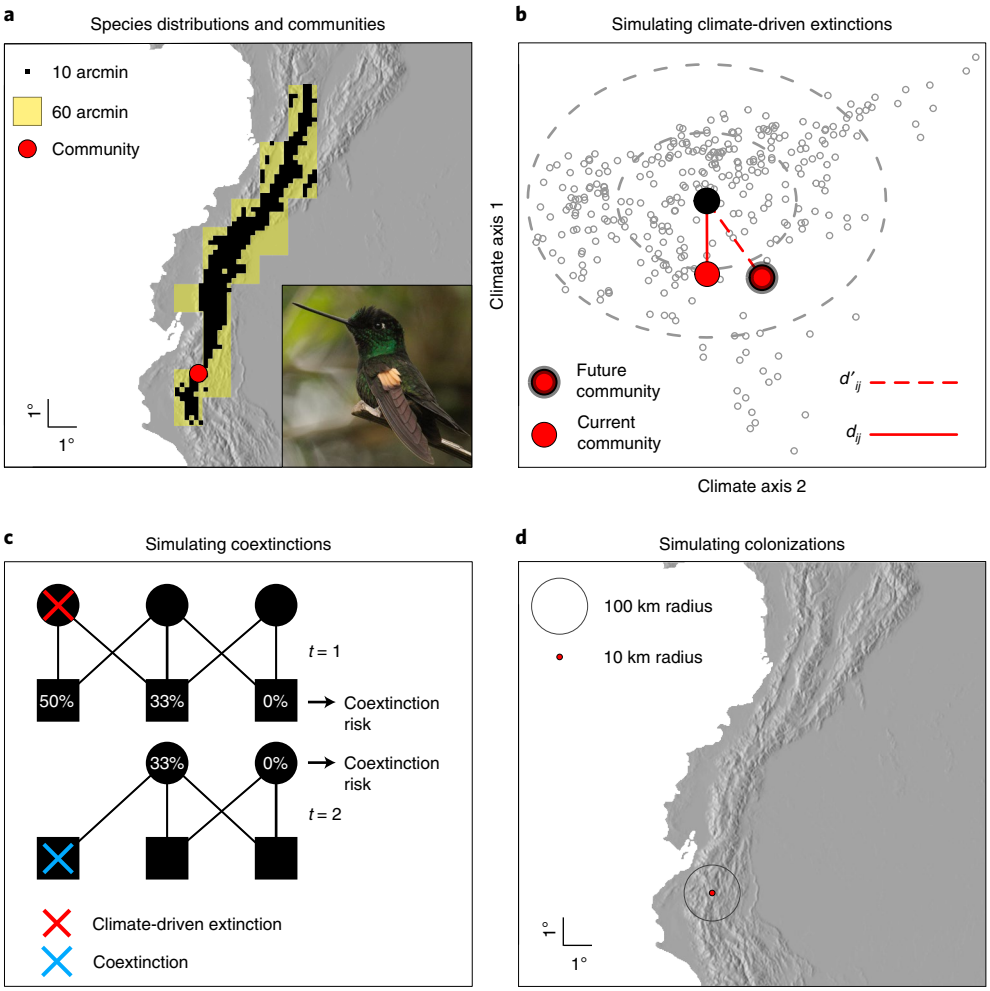

Fig. 1 | Conceptual figure illustrating our simulations of climate-driven extinctions, coextinctions and colonizations. a, Species distributions and communities: beginning with the information on hummingbird geographical distributions, exemplified by a hummingbird species from the High Andes *Coeligena lutetiae*. The red point marks the location of a network in which the species was recorded. The yellow grid shows the species' breeding distribution at 60 arcmin resolution. We then projected the species' distribution onto a digital terrain model in 10 arcmin resolution (344 km^2 at Equator) and removed grid cells falling outside the species elevational range limits (black grids). **b**, Simulating climate-driven extinctions: from the black coordinates in **a**, we extracted the variables that were used to characterize the species' climate volume (grey points). The large black dot marks the centroid of the species' estimated climate volume, based on its breeding distribution. The ellipses mark one and two standard deviation distances from that climate centroid. The large red dots represent the climate conditions in the focal network *j*. The solid red line shows the standardized distance (*z*-score) to the network's current climate conditions (d_{ij}) and the dashed red line shows the standardized distance to the network's future climate conditions (d'_{ij}). With these *z*-scores, we calculate the proportion of the *i*th species' climate volume that takes values within ($d'_{ij} - d_{ij}$) and d'_{ij} standard deviations from the climate volume's centroid. These proportional values give the 'climate change impact' and the 'future climate mismatch', respectively. These two probabilities were multiplied to obtain a species' climate-driven extinction risk. If $d'_{ij} < d_{ij}$, we assumed the extinction probability to be zero. **c**, Simulating coextinctions: the local climate-driven extinction of the species can cause cascades of coextinctions within plant–hummingbird interaction networks. The network illustrates interacting hummingbirds (circles) and plants (squares) over two simulation iterations. At the first iteration ($t = 1$), climate change causes the loss of one hummingbird species and the probability of plant partner coextinctions is modelled as proportional to the fraction of lost interactions. At the second iteration ($t = 2$), the coextinction cascade reaches the hummingbirds. The coextinction cascade stops when an iteration *t* produces no coextinction events. **d**, Simulating colonizations: lastly, we simulate colonization from a regional source pool. The pool of potential colonists consists of all hummingbird species occurring within a given buffer radius around the focal network. We simulated colonization probability of a source pool species *i* as the proportion of its climate volume falling beyond d'_{ij} standard deviations from the climate volume's centroid. Therefore, the colonization probability was not influenced by the extinction events and vice versa.

standard deviations from the climate volume's centroid. These *z* scores give, respectively, the 'climate change impact' and the 'future climate mismatch'. We multiplied these two proportions to obtain a species' climate-driven extinction risk. As such, the climate-driven extinctions depend on the amount of climate change and how well the future climate is represented in species' contemporary ranges. When d_{ij} exceeded d'_{ij}, we assumed the extinction risk to be zero.

In the third stage, we simulate coextinctions with probabilities given by the proportion of interactions lost by each species (Fig. 1c). Coextinction cascades were initiated by climate-driven extinctions of hummingbirds but could subsequently result from other coextinctions, due to loss of interactions. Our first coextinction simulations assumed strict dependence between mutualistic partners, corresponding to a 'worst case' coextinction scenario.

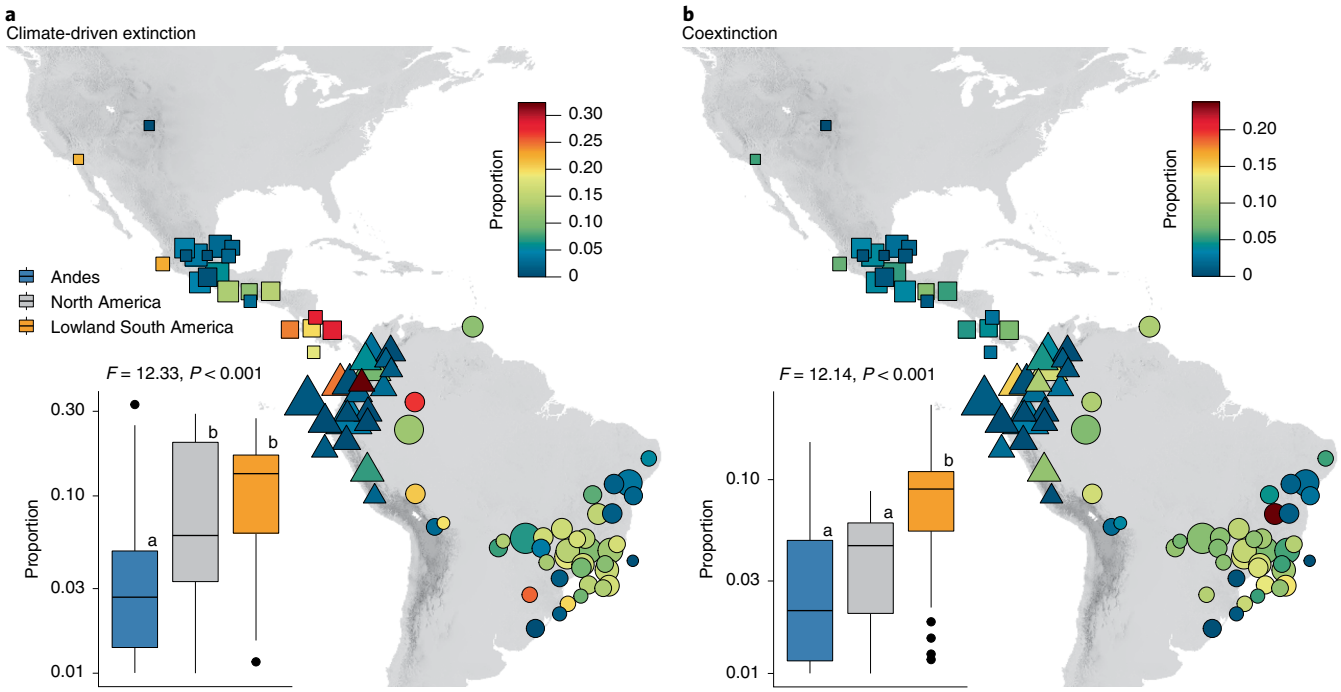

Fig. 2 | The geographic patterns of local climate-driven extinction and coextinction across the Americas. a,**b**, Biogeographical variation in climate-driven extinctions (**a**) and coextinctions (**b**), measured as the average proportion of hummingbirds in our simulations that disappeared from the networks. Point types represent the three biogeographical regions: North America (squares), Andes (triangles) and lowland South America (circles). Point sizes are proportional to the number of hummingbird species in each network. Some points have been slightly moved for visualization purposes. The *F*-statistics derive from one-way ANOVA testing for regional differences in climate-driven extinctions ($F = 12.33$, $P < 0.001$, $n = 84$) and coextinctions ($F = 12.14$, $P < 0.001$, $n = 84$). Both extinction variables were scaled on logarithmic axes. The lower-case letters represent the statistical difference according to Tukey multiple comparisons with Bonferroni-adjusted *P* values ($P < 0.05$). The box borders mark the interquartile range (IQR; quartiles 1 to 3); horizontal lines inside boxes mark the medians; vertical lines mark ±1.5× IQR; circles mark data outliers. The results derive from the RCP 4.5 'mid-range' scenario for the year 2070.

Subsequently, we repeated the coextinction simulations by allowing species to relocate 50% of their lost interactions with remaining partners in the network, following the 'constrained rewiring model' in Schleuning et al.[8].

Lastly, we simulate hummingbird colonizations by sampling species from a 100 km buffer zone, reflecting species dispersal distances at the temporal scale of decades (Fig. 1d). The 100 km radius could overestimate the local source pools if intersecting topographic dispersal barriers. Hence, we repeated the colonization analyses using a more conservative dispersal distance of 10 km. We calculated the colonization probability of a source pool species as the proportion of its climate volume falling beyond d'_{ij} standard deviations from the climate volume's centroid (see Methods for more details regarding each simulated process).

We use the simulated patterns of climate-driven extinctions, coextinctions and colonizations to pinpoint regions where communities are most vulnerable to future climate changes. We expect that the Andean communities are least vulnerable to future climate change because the topographically heterogeneous landscape has a buffering effect on climate-driven dynamics in species' ranges[22,23]. Moreover, the Andean ecoregion has a large pool of potential colonists, which could balance against local extinctions[24]. Consequently, we expect Andean communities to have low climate-driven extinction and coextinction rates but high colonization rates. By contrast, the lowland parts of South America are predicted to experience drastic climate changes in the future[25–27], more so than they experienced during the Last Glacial Maximum[22]. Therefore, we expected communities in lowland South America to be most vulnerable to climate-driven extinctions followed by North American communities.

The geographical pattern of coextinctions depends primarily on the climate-driven extinction rate: the more species and interactions that disappear by climate-driven extinctions, the more coextinctions could impact the community's remaining species. However, we also expected coextinction rates to depend on intrinsic properties related to network configuration. Firstly, there could be a bias in climate-driven extinctions towards specific network roles—notably, if climate-driven extinctions remove generalized species with many interactions, coextinctions could spread throughout the network[28,29]. Here, we use each species' 'effective number of partners' to measure how generalized species are in the networks[8,30]. Specifically, we trace the cumulative effective partner number lost by each climate-driven extinction simulation.

While losing generalized species to climate-driven extinctions increases the initial coextinctions, the network's overall structure may affect the degree to which coextinctions spread to other species[17,31–33]. For instance, specialized network structures may be robust against coextinctions as there is little overlap between the species' foraging niches. In a specialized network, a pollinator may be vulnerable to losing its mutualistic partners but it should be little affected by the loss of other species' partners[32,34]. Therefore, increased specialization within communities may reduce the cascading spread of coextinctions. Here, we measure community-level specialization by two indices: complementary specialization[35] and modularity[36]. Complementary specialization measures the partitioning of interactions among pollinators and plants relative to a null model that assumes that species interact randomly according to partner availability. The modularity index measures the extent to which pairwise interactions are clustered into modules of

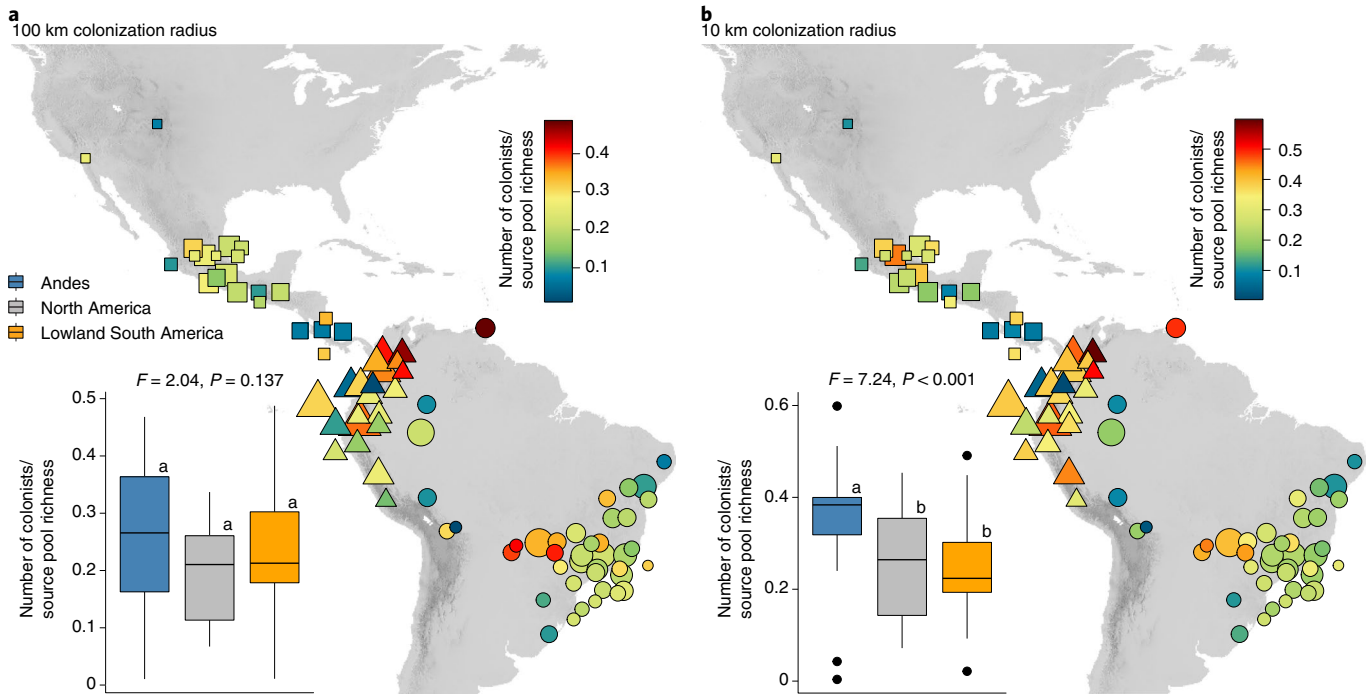

Fig. 3 | The geographic patterns of local colonization across the Americas. a,**b**, Biogeographical variability in colonization rates, measured as the average number of hummingbird colonists relative to the species richness within a source pool radius of 100 km (**a**) and 10 km (**b**). Point types represent the three biogeographical regions: North America (squares), Andes (triangles) and lowland South America (circles). Point sizes are proportional to the number of hummingbird species in each network. Some points have been slightly moved for visualization purposes. The *F*-statistics derive from one-way ANOVA testing for regional differences in colonization rates (100 km radius—$F = 2.04$, $P = 0.137$, $n = 84$; 10 km radius—$F = 7.24$, $P < 0.001$, $n = 84$). Lower-case letters represent the statistical difference according to Tukey multiple comparisons with Bonferroni-adjusted *P* values ($P < 0.05$). The box borders mark the IQR (quartiles 1 to 3); horizontal lines inside boxes mark the medians; vertical lines mark ±1.5× IQR; circles mark data outliers. The results derive from the RCP 4.5 'mid-range' scenario for the year 2070.

mutualistic partners. Thereby, the two indices represent two conceptually different approaches to quantifying resource partitioning in mutualistic networks, although they might be correlated. The literature also highlights nestedness as a structure contributing to network robustness through a large overlap in interactions[31,37]. The nested structure characterizes a core of interacting generalists, while the specialized species' interactions nest within generalized partners. Removing a specialist from such a network will impact only a small proportion of the generalized species' interactions, which minimizes the chance for coextinction to spread throughout the network[31,37]. Therefore, after running the simulations, we examine (1) if there is a bias in climate-driven extinctions towards generalized network roles and (2) if specific network structures (that is, complementary specialization, modularity and nestedness) influence the geographical patterns of coextinctions.

Results

The geographic patterns of local extinction (Fig. 2) and colonization (Fig. 3) showed marked differences across the Americas. Notably, North American and lowland South American communities experienced more climate-driven extinctions than Andean communities (Fig. 2a). On the other hand, coextinction rates were significantly more frequent in the South American lowlands than in both the Andes and North America (Fig. 2b). While Andean communities experienced few extinctions overall, they received more colonists than the other regions (Supplementary Fig. 5), making Andean communities more robust to climate change than the rest of the mainland Americas. The Andes' large number of colonists in Supplementary Fig. 5 reflected a high total species richness within a 100 km source pool radius around each community (Fig. 3a). However, the robustness of Andean communities was confirmed when reducing the colonization radius to 10 km. Here, Andean communities had the highest colonization rates relative to the local source pool's species richness (Fig. 3b). These results were simulated according to the representative concentration pathway RCP 4.5 'mid-range' future climate scenario and were consistent in the RCP 8.5 'worst case' future climate scenario (Extended Data Figs. 1–4).

In both RCP scenarios, we found a reduced spread of coextinctions in North American networks, considering the number of species lost to climate-driven extinctions (Fig. 4a). This pattern reflected a bias in climate-driven extinctions against species with generalized network roles (Fig. 4b). Relative to the proportion of climate-driven extinctions, North American communities lost fewer generalized species than communities in the Andes and lowland South America (examples in Fig. 5). To relax the assumption of complete dependency between hummingbird and plant species, we repeated our coextinction simulations by allowing species to relocate 50% of their lost interactions with remaining partners. While the interaction rewiring reduced the overall coextinction rate, the biogeographical patterns remained robust (Extended Data Figs. 5–7): the coextinction rates were higher in lowland South America compared to the Andes and North America (Extended data Fig. 5). Moreover, coextinctions spread slowest in North America, considering the proportion of climate-driven extinction (Extended Data Fig. 6).

As expected the degree of complementary specialization and modularity were strongly correlated (Pearson's $r = 0.78$, $P < 0.001$, $n = 84$). Both metrics were indistinguishable between regions (Extended Data Fig. 8) and, thus, did not explain the regional differences in coextinction. Nevertheless, complementary specialized

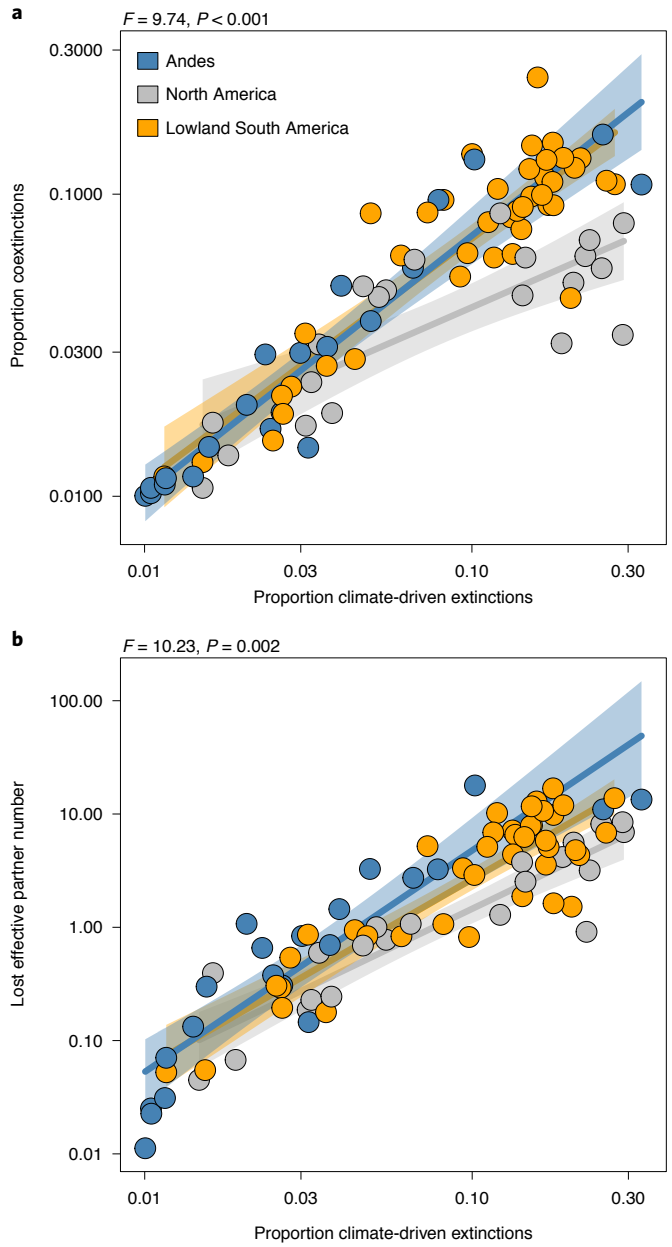

Fig. 4 | Biogeographical variability in the communities' vulnerability to coextinctions after accounting for climate-driven extinctions. **a**,**b**, Coextinctions spread less in North America compared to other regions (**a**, $F = 9.74$, $P < 0.001$, $n = 83$), which coincides with a regional bias in climate-driven extinctions against species with generalized network roles (**b**, $F = 10.23$, $P = 0.002$, $n = 83$). Each F-test compares two linear regression models, of which one contains the biogeographical region as a character state predictor variable. The species-level generalism was described by the effective number of partners. The y axes measure the cumulative lost partner number averaged across the simulations, thereby illustrating the loss of species-level generalism. The solid lines represent the linear relationships within each region (with shaded 95% confidence intervals). The results depicted here derive from the RCP 4.5 'mid-range' scenario for the year 2070.

and modular network structures reduced the effects of coextinctions among all networks (Fig. 6). Relative to the proportion of climate-driven extinctions, we found few coextinctions in the most complementary specialized and modular networks (Fig. 6a,b). By contrast, the level of nestedness did not affect coextinction spread (Fig. 6c).

These results were consistent within regions except the Andes, where the low climate-driven extinction rates were too low to detect the buffering effect of complementary specialized and modular network structures (Supplementary Table 3). Moreover, the results were consistent when including interaction rewiring into the coextinction simulations (Extended Data Fig. 7). Our simulations of climate-driven extinctions and colonizations were based on climates extracted from the hummingbirds' breeding distributions. For this reason, we excluded boreal migrants from tropical networks located outside the species' breeding ranges (Supplementary Table 2). This operation made the networks smaller than initially sampled, which also affected network structure. Nevertheless, the results were similar when excluding (Fig. 6) or including (Supplementary Fig. 6) boreal hummingbird migrants when calculating network structure.

Discussion

Our simulations showed strong geographic patterns in the communities' vulnerability to local extinctions (Fig. 2) and rates of colonizations (Fig. 3). High colonization rates did not equally compensate for high extinction rates across biogeographical regions. Instead, colonizations from regional source pools were highest in Andean communities that were already least vulnerable to local extinctions. On the other hand, communities from the South American lowland experienced many climate-driven extinctions and coextinctions but few colonizations. Thus, colonizations from the regional source pools may not adequately compensate for species loss in the South American lowland, the most vulnerable region.

In alignment with our initial expectations, the communities with the lowest climate-driven extinctions occurred in the Andes (Fig. 2a). The Andean mountains combine climate stability with topographic complexity, enabling species to track optimal climate conditions by dispersing short distances along the slope[22,23]. In such environments, future climate changes may have limited effects on the species range dynamics, increasing the chance for communities to maintain their structural integrity. By contrast, lowland South America may experience the most drastic future climate change among the Neotropical biomes[25–27]. The area's homogeneous topography, compared to the Andes, entails that species must disperse longer distances to conserve their climate niches[23]. In the process, local communities may experience high turnover in species composition and disruption of interspecific interactions, as species track climates with different speeds[12].

Andean communities received the highest number of colonists from a radius of 100 km (Supplementary Fig. 5), although this pattern disappeared when standardizing for the source pool's species richness (Fig. 3a). Due to topographic barriers and diverse climate zones[38–40], the species' dispersal could happen over much smaller distances. Thus, we repeated the analysis with a more conservative colonization radius of 10 km and found Andean communities had the highest colonization rates relative to the source pool's species richness (Fig. 3b). This result suggests that high colonization rates in Andean communities were not solely derived from their species-rich source pools. Instead, Andean communities may receive more colonists as a consequence of future climate suitability. Both the extinction and colonization simulations include contemporary and future climate data but had otherwise no impact on each other. Hence, the simulations contain two lines of evidence suggesting that Andean communities are most resilient to future climate changes. Nevertheless, high colonization rates in the Andes do not imply overcompensation for extinctions. Apart from climate suitability, actual species establishments depend on several local factors and processes that we cannot account for in the simulations, such as resource availability and interspecific competition. Moreover, interspecific variation in dispersal abilities may impact species'

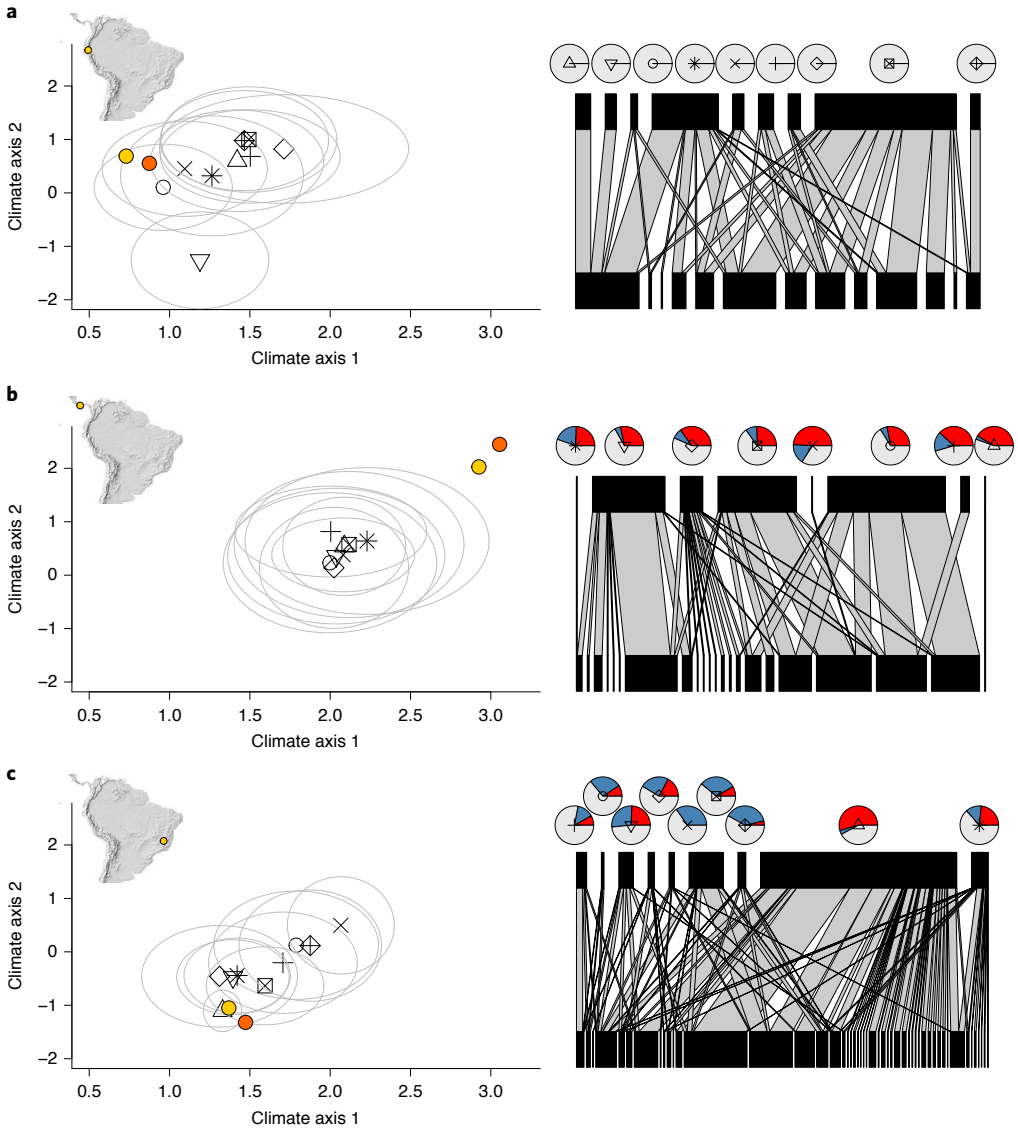

Fig. 5 | Three examples of climate-driven extinction and coextinction, characteristic for each biogeographical region. a–c, The scatterplots show the climate volumes for hummingbird species in three communities. Black symbols and grey ellipses, respectively, mark the centroid and standard deviation of each species' climate volume. Yellow and orange points, respectively, mark the current and future climate conditions in the community. The network diagrams illustrate the interactions between hummingbirds (upper black boxes) and plants (lower black boxes). The widths of the boxes are proportional to the species' total number of interactions. The widths of the connecting lines are proportional to species pairwise interaction frequencies. Pie diagrams associated with each hummingbird depict the proportion model replicate in which the species went locally extinct due to climate (red) or due to coextinctions (blue). **a**, An Andean network with a low climate-driven extinction rate and consequently a low coextinction rate. **b**, A network from Costa Rica with high climate-driven extinction but a low coextinction rate. **c**, A Brazilian network where most species have low climate-driven extinction risk, except a highly generalized species (upward triangle). Losing this species could trigger coextinctions of species throughout the network.

occupancy of climatically suitable communities. Accounting for dispersal differences is challenging for simulation studies as dispersal is one of the biological processes we know least about—particularly for the tropical avifauna[41]. As such, the simulated colonization process should be viewed as a colonization potential rather than species establishing in the community.

Although North American communities experienced similar rates of climate-driven extinction as communities from the South American lowland, they had disproportionally fewer coextinctions (Fig. 4a). The reason was that climate-driven extinctions impacted few generalized species in North American networks (Fig. 4b). When climate-driven extinctions mainly impact species in the network's periphery, it will result in few coextinctions[28] (Fig. 5b). However, coextinction spread increases when communities lose generalized species, as these have many mutualistic partners distributed throughout the network (Fig. 5c). These results illustrate the importance of network roles when assessing climate change pressures on ecological communities. Notably, the generalized species with interactions connected throughout the network could be considered keystones for a community's resilience against climate change[28]. These species appeared less impacted by climate-driven extinctions in North America; hence, the networks maintained most of their structural integrity. Why climate-driven extinction impacts peripheral network roles in North American communities remains an open question. North American hummingbird communities are dominated by one hummingbird group, the so-called

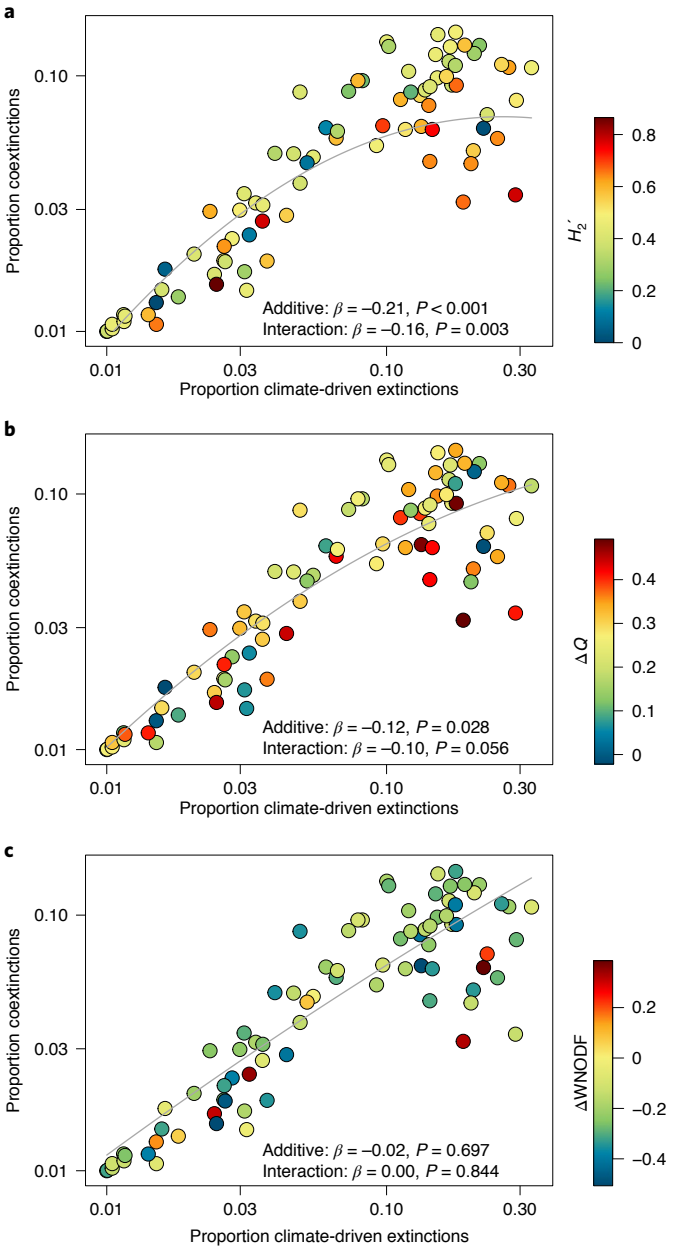

Fig. 6 | The influence of three network structures on the logarithmic association between climate-driven extinctions and coextinctions ($n = 83$). a–c, The three network structures are complementary specialization (H_2'; **a**), modularity (ΔQ; **b**) and nestedness (ΔWNODF; **c**). Trend lines and standardized coefficients derive from weighted multiple linear regressions. In each regression model, we added an interaction term between the proportion of climate-driven extinctions and the network metric. The weights were given by the number of hummingbird species sampled in each network. All results depicted here derive from the RCP 4.5 'mid-range' scenario for the year 2070.

'Bees', which is a recently derived and rapidly diversifying lineage with generalized foraging niches[21,42]. Moreover, the lineage represents the hummingbird's only successful colonization of the temperate North Americas. Consequently, the Bees may have more adaptable climate niches compared to the older tropical lineages. Hence, the North American networks may have a core of generalized hummingbirds with broad climate niches that persist under climate change.

While the species' network roles affected the initiation of coextinctions, the spreading of coextinctions to other species was influenced by network-level complementary specialization and modularity[32,34]. Since species are more isolated in specialized and modular networks, they should be less affected by other species' lost interactions—although they are more vulnerable to losing their own mutualistic partners. Therefore, a high degree of specialization and modularity at the network level could prevent the spreading of coextinctions[32,34]. Accordingly, we found that networks with more specialized and modular structures suffered fewer coextinctions than generalized networks (Fig. 6a,b). By contrast, we found no effect of nestedness on the networks' resilience to coextinction (Fig. 6c). In general, nested networks are highly cohesive, lowering the risk of species becoming isolated in the network after perturbations[31,37]. However, when climate-driven extinctions remove the core of generalized species, coextinctions can spread quickly throughout the network. Thus, in line with previous theoretical work[29], the stabilizing role of nestedness depends on which species are driven to extinction. Suppose climate-driven extinctions primarily impact species with generalized network roles. In that case, nestedness could theoretically decrease network resilience[29]. Opposite, the isolation of interactions in specialized and modular structures should buffer against perturbations even if generalized and centrally connected species disappear.

The results from our simulations contribute to the recent literature joining climate niche modelling and biotic interactions[8,9]. As for similar simulation-based studies, there are obvious caveats worth mentioning. Firstly, species could be absent from climatically suitable habitats due to dispersal limitations and barriers. Thus, the climate volume estimated from the species' distributions may constitute only a subset of the fundamental niche. Moreover, some hummingbird–pollinated plants attract other types of pollinators, notably insects or bats[43]. Such generalist plants may not disappear from a community if their hummingbird pollinators go extinct[17]. These caveats imply that simulations are likely to overestimate species loss and that the extinction patterns may not necessarily reflect real extinctions but rather loss in species fitness[17]. Nevertheless, our simulations solely rely on climate conditions while ignoring land-use change and climate-driven extinctions in the plant community. Consequently, we may not have depicted a worst-case scenario in local extinctions (or fitness loss). To improve the simulations, one would need better data on tropical plant distributions and estimated future land-use changes.

Taken together, we have combined biotic interactions and species climate volumes to predict how biological communities respond to climate change across biogeographical regions. The interdependency between species that defines biological communities offers an additional angle for climate changes to impact species. As such, the coextinction concept implies that species in mutualistic networks would be more vulnerable to climate changes than anticipated by climate niche models[9]. At the same time, colonizations from regional source pools may contribute to a community's resilience by compensating for local extinctions. Hence, local climate-driven extinctions, coextinctions and colonizations represent distinct processes affecting biological communities under climate change. Our study contributes by integrating these processes into the same analytical framework. Notably, the increased realism of the models achieved by considering biotic interactions generates novel biogeographical patterns that would otherwise remain hidden. These unique patterns in the communities' vulnerability to interaction loss should inspire future research avenues provided by the increased availability of ecological network data.

Methods

Plant–hummingbird interaction networks. We used 84 weighted hummingbird–plant interaction networks published in Dalsgaard et al.[21]. The networks contain field observations of hummingbirds visiting flowering plants within localities

distributed across the American mainland (39° N–32° S). Each network is presented as P (number of plant species) × H (number of hummingbird species) matrices with quantitative entries that indicate the interaction frequencies between each hummingbird and flowering plant species. The networks sampled only mutualistic interactions in which the hummingbird extracted nectar while touching the reproductive structures. In total, the database sampled 169 hummingbird species and 1,201 plant species on the mainland Americas. Compared to the published database, we excluded nine Caribbean island networks (11 hummingbird species and 55 plant species). On islands, area and isolation strongly influence species assembly, making the extinction–colonization dynamics non-analogous to the mainland[44–46]. Moreover, island species usually have small ranges constrained by the sea rather than climate, which complicates climate niche modelling[47].

Quantifying network structures. We calculated the following three network metrics: complementary specialization[35], quantitative modularity[36] and weighted nestedness[48]. All three structures have properties hypothesized to influence network stability[8,31,49,50]. Complementary specialization (H_2') quantifies the partitioning of interactions among pollinators and plants relative to a null model that assumes species interact randomly according to partner availability, thus reflecting the degree of resource partitioning between species. The modularity index Q quantifies the extent to which networks are clustered into modules of preferentially interacting species. Q was calculated for each network using the DIRTLPA + algorithm, which is specifically designed to search for modules within quantitative bipartite networks[51]. Weighted nestedness (WNODF), characterizes a structure with a core of interacting generalists, while the specialized species' interactions are nested within generalized partners. All three metrics range between 0 and 1, where larger values indicate, respectively, high degree of complementary specialization (plants have many interactions with hummingbirds that are not shared with other species in the guild), high degree of modularity (strong tendency of species to form subgroups within the network) and a high degree of nestedness (strong tendency of specialized species to interact with more generalized partners).

Because networks vary in species richness and sampling effort, measurements of network structure are often not directly comparable[37]. To account for these confounding effects, we applied null models, which calculate each network metric after a random shuffling of interactions. Following Sonne et al.[52], who evaluated different null models, we used Patefield's algorithm, which constraints the total interaction frequency of each species[53]. We then subtracted the empirical network structure from the null model's mean obtained from 1,000 randomizations (that is, Δ transformation, following ref. [54]). Because the raw values of H_2' are already corrected for the marginal totals of the network, we only applied the null model correction to Q and WNODF. All network analyses were conducted in R using the 'bipartite' package v.2.11 (ref. [55]).

Hummingbird geographical distributions. Information on the hummingbird's geographical breeding range consisted of 60 arcmin resolution presence–absence maps for the 339 extant mainland species, following the International Ornithological Committee World List (IOC v.10.1; www.worldbirdnames.org). The data are an updated version of the database presented initially in Rahbek and Graves[19,20]—see supplementary material in Holt et al.[56]. These distributional data were supplemented with information on global recorded minimum and maximum elevations for each hummingbird species (Supplementary Sources). We combined the geographical distribution and the altitude range limits to predict the hummingbirds' distributions onto a digital terrain model in 2 arcmin resolution National Geophysical Data Center[57]. A hummingbird species was considered present in a 2 arcmin grid cell if it overlapped with both its distribution at the 60 arcmin scale and its altitudinal range limit (Fig. 1a). Particularly for High Andean species, this operation determined range sizes to be notably smaller than the projection at 60 arcmin resolution. Finally, to minimize omission errors (when a species is falsely thought to be absent), we aggregat the species' distribution at 2 arcmin resolution to 10 arcmin resolution (344 km² at the Equator).

Estimating hummingbird climate volumes. To simulate local climate-driven extinctions and colonizations (see below), first, we estimated the occupied climate volume of all 356 extant hummingbird species. We based the climate volume on four bioclimatic variables relevant for bird distributions[19,20,58–61]. Low climate seasonality is one of the most important characteristics of tropical latitudes and has also been associated with high avian species richness[59,61]. Thus, we included commonly used measures of annual climate seasonality in temperature (standard deviation × 100) and precipitation (coefficient of variation). Also relevant for bird distributions are the broadly accepted correlations between global richness patterns and water–energy-related climate variables[19,20,58,60]. To capture these variables, we included mean annual temperature and annual precipitation. All climate variables were extracted from the CHELSA climate database in 10 arcmin resolution[62] (https://chelsa-climate.org). The four climate variables were combined into major orthogonal axes using principal component analysis. We kept the first two principal components (PCs), which captured 86% of the climate variation across the entire Americas (PC1 = 56%, PC2 = 30%). We characterized each hummingbird species' occupied climate volume by the mean and standard deviation of PC1–2 extracted from the species' breeding range (Fig. 1b). To avoid issues with poor model reliability at small sample sizes[63], we excluded species represented by less than ten climate samples at the 10 arcmin resolution (six species, none of which were in the networks).

Simulating climate-driven extinctions and coextinctions. We simulated local hummingbird extinctions as a two-stage stochastic process, following the procedure proposed by Bascompte et al.[9] (Fig. 1c). At the first stage, we simulated the risk of local extinctions of all hummingbird species due to future climate changes. At the second stage, we simulated the potential coextinction cascades that followed the climate-driven extinction events.

To simulate the local extinction risk of hummingbird species as a direct consequence of future climate changes, we used the conceptual framework in Blonder et al.[64]. First, the algorithm defines a species' current climate mismatch (d_{ij}) as the standardized distance (z-score) between the current climate extracted network i's locality and the centroid of species j's climate volume. Then, the algorithm compares a species' climate volume with the network's future climate. For this purpose, we compiled the future climate at each network location as predicted by a broad range of general circulation models (Supplementary Table 1). We considered two RCPs: a worst-case scenario, which assumes a continuous rise in greenhouse gas emissions throughout the twenty-first century (RCP 8.5) and a more optimistic scenario, which assumes a stabilization in greenhouse emissions after the year 2070 (RCP 4.5). With these data, we defined the future climate mismatch (d'_{ij}), as the number of standard deviations separating the future climate of network i from the centroid of the species j's climate volume. Subtracting d'_{ij} from d_{ij} gives the climate change within a network locality relative to the climate volume of species j—that is, the 'future climate impact'. The 'future climate mismatch' and 'future climate impact' were converted to probabilities by taking the proportion of the climate volume that takes values within ($d'_{ij} - d_{ij}$) and d'_{ij} standard deviations from the climate volume's centroid (Supplementary Figs. 1–4).

Regardless of climate change, species may persist if the local climate remains engulfed by their occupied climate volume. Hence, we modelled the climate-driven extinction risk of hummingbird j in network i as the product between the 'future climate mismatch' and 'future climate impact'. In this way, climate-driven extinctions depend on the amount of climate change and how well the future climate is represented in species' contemporary ranges—Supplementary Figs. 1–4 provide a more detailed description. In cases where d_{ij} exceeded d'_{ij}, we assumed the climate-driven extinction risk to be zero. Since we estimate climate-driven extinction risks based on the species' breeding distributions, we excluded boreal migrants from networks located outside their breeding ranges (Supplementary Table 2). This operation made the networks smaller than initially sampled, which also affected network structure. Therefore, we calculated the three network structures (H_2', Q and WNODF) before and after excluding the boreal migrants.

During the climate-driven extinction simulations, we tracked the species names and generalization levels of the lost hummingbirds. If the lost species have generalized network roles, there is an increased risk for the remaining species to be impacted by coextinctions[28]. To quantify the species' network roles, we calculated the species' effective number of partners following Schleuning et al.[8]. This metric describes species' generalization level as a measure of niche breadth (based on Shannon's H), corresponding to the actual partner number if each edge were observed equally frequently[30]. Losing a generalized species with high partner diversity could result in a rapid spread of coextinctions throughout the network. Thus, we calculate the loss of species generalization level as the total effective partner number lost after each simulation replicate. The generalization measure was calculated using the 'species level' function from the 'bipartite' package v.2.11 (ref. [55]).

Proceeding to our simulations' second stage, we define the coextinction risk by the proportion of interactions lost by each species. In our simulations, coextinctions are first triggered by climate-driven extinctions of hummingbirds in a focal network. The coextinctions then spread stepwise at each iteration t. At iteration $t = 1$, plants' coextinction probability is proportional to the fraction of interactions lost by hummingbird climate-driven extinctions. At $t = 2$, hummingbird coextinction probability is proportional to the fraction of interactions lost by plant coextinction at $t = 1$. Thereby, for a given network, the coextinction probability of species z (hummingbird or plant) at iteration t is given by $c_t^z = 1 - (I_t^z / I_{t-1}^z)$, where I_t^z is the remaining interaction frequency of species z at iteration t and I_{t-1}^z states the interaction frequency of species z at the beginning of $t-1$ (ref. [9]). The algorithm stops after the first time it samples zero coextinct species. The simulation ran over 1,000 replicates for each network ($n = 84$), RCP climate scenario ($n = 2$) and general circulation models ($n = 32$). For each group of 1,000 replicates, we calculated the mean proportion of locally extinct hummingbird species at stage one (climate-driven extinctions) and stage two (coextinctions). The simulations were conducted only for the networks' hummingbirds. Although the simulations would also be relevant for plants[17], there is no equally detailed and up-to-date information on plant geographic ranges.

So far, the coextinction simulations rely on a crude assumption of strict mutual dependencies, that is a species disappears from a network if it loses all its interactions. We tested the sensitivity to this assumption by subsequently allowing species to relocate 50% of their lost interactions, in each extinction step, to their remaining partners in the network. This model follows the 'constrained

rewiring' from Schleuning et al.[8]. We acknowledge that climate-driven disruption of interactions may also force species to find new mutualistic partners and thereby avoid coextinction[17,65]. As such, our simulated coextinctions may not reflect real extinctions but rather reductions in the species' fitness. Thus, the network simulations are an appropriate tool for assessing the communities' vulnerability to mutualistic partner loss[16,17] and may illustrate the worst-case scenario of species' response to climate change.

Simulating regional colonization. We simulated hummingbird colonizations independently of the extinction simulations. Given the short time frame between the current and future climate projections, we assumed dispersal to occur exclusively at the regional scale. Specifically, we defined the source pool of a focal network as the species with breeding distributions within a radius of 100 km (Fig. 1d). We repeated the analyses for a 10 km buffer radius, corresponding to a more conservative source pool definition.

We defined the colonization probability of hummingbird j into network i as the proportion of j's climate volume falling beyond d'_{ij} standard deviations from the climate volume's centroid. The simulation was repeated 1,000 times for each network ($n=84$), RCP climate scenario ($n=2$) and general circulation models ($n=32$). Thus, we analysed a total of 1,000 replicates for each 32 general circulation model giving 32,000 simulations for each network. On the basis of the 1,000 simulated replicates, we calculated the mean number of colonizing hummingbird species relative to the richness of hummingbirds in the network and relative to the source pools' species richness.

Statistical analyses. The 32 general circulation models generate different results of climate-driven extinction, coextinction and colonization. Thus, we calculated the mean across the 32 values of climate-driven extinction, coextinction and colonization rates for each network. Following Dalsgaard et al.[21], the mainland networks were grouped into three biogeographical regions: the Andes ($n=21$), South American lowlands ($n=41$) and North America ($n=22$). The Andean region includes all networks within the tropical High Andes and its foothills according to the mountains polygons published in Rahbek et al.[66]. The North American region includes all mainland networks north of the Panamanian Isthmus. The South American lowland includes the remaining continental networks in South America. Before statistical analyses, we log-transformed both the rates of climate-driven extinction and coextinction to improve normality. We tested for biogeographical variability in climate-driven extinction, coextinction and colonization by weighted analysis of variance (ANOVA). The weights were given by the number of hummingbird species sampled in each network, assuming that estimates from species-rich networks are more reliable than estimates from species-poor networks. We subsequently conducted Tukey multiple comparisons with Bonferroni-adjusted P values to determine which regions were most distinct in terms of climate-driven extinction, coextinction and colonization. The post hoc analyses were performed in R by the general linear hypotheses function glht from the 'multcomp' package v.1.4.16 (ref. [67]). We then tested if the correlation between climate-driven extinction and coextinction differed between biogeographical regions. To do so, we regressed the proportion of coextinctions against the proportion of climate-driven extinctions. We then fitted a second model, including biogeographical region as a character state predictor variable. The two models, with and without the biogeographical predictor, were then compared statistically using an F-test.

We then assessed if the three network metrics correlated with the spread of coextinction events when considering the proportion of climate-driven extinctions. The logarithmic relationship between climate-driven extinction and coextinction was refitted with a network metric and interaction term added as predictor variables. As previously, the regression weights were given by the networks' richness of hummingbird species. A regional bias in vulnerable network roles could interfere with coextinction's dependency on network structure. Hence we also fitted the regressions individually for each region. Moreover, we repeated the analysis keeping boreal migratory hummingbirds in the networks when calculating H_2', ΔQ and ΔWNODF. One network from North America experienced no climate-driven extinctions (and consequently coextinctions) across all simulations. Hence, it was excluded when analysing the factors influencing coextinction spread.

Reporting Summary. Further information on research design is available in the Nature Research Reporting Summary linked to this article.

Data availability

Data used to conduct the analysis are provided at the figshare repository: https://doi.org/10.6084/m9.figshare.19071752.v2

Code availability

The Methods contains a detailed description of our analytical framework. R codes in the simulations are provided at the figshare repository: https://doi.org/10.6084/m9.figshare.19071752.v2

Received: 25 June 2021; Accepted: 7 February 2022;
Published online: 28 March 2022

References

1. Schemske, D. W. in *Foundations of Tropical Forest Biology* (eds Chazdon, R. L. & Whitmore, T. C.) 163–173 (Univ. Chicago Press, 2002).
2. Hooper, D. U. et al. Effects of biodiversity on ecosystem functioning: a consensus of current knowledge. *Ecol. Monogr.* **75**, 3–35 (2005).
3. Schemske, D. W., Mittelbach, G. G., Cornell, H. V., Sobel, J. M. & Roy, K. Is there a latitudinal gradient in the importance of biotic interactions? *Annu. Rev. Ecol. Evol. Syst.* **40**, 245–269 (2009).
4. Schweiger, O., Settele, J., Kudrna, O., Klotz, S. & Kühn, I. Climate change can cause spatial mismatch of trophically interacting species. *Ecology* **89**, 3472–3479 (2008).
5. Hegland, S. J., Nielsen, A., Lázaro, A., Bjerknes, A.-L. & Totland, Ø. How does climate warming affect plant–pollinator interactions? *Ecol. Lett.* **12**, 184–195 (2009).
6. Walther, G.-R. Community and ecosystem responses to recent climate change. *Philos. Trans. R. Soc. B* **365**, 2019–2024 (2010).
7. Blois, J. L., Zarnetske, P. L., Fitzpatrick, M. C. & Finnegan, S. Climate change and the past, present and future of biotic interactions. *Science* **341**, 499–504 (2013).
8. Schleuning, M. et al. Ecological networks are more sensitive to plant than to animal extinction under climate change. *Nat. Commun.* **7**, 13965 (2016).
9. Bascompte, J., García, M. B., Ortega, R., Rezende, E. L. & Pironon, S. Mutualistic interactions reshuffle the effects of climate change on plants across the tree of life. *Sci. Adv.* **5**, eaav2539 (2019).
10. Memmott, J., Craze, P. G., Waser, N. M. & Price, M. V. Global warming and the disruption of plant–pollinator interactions. *Ecol. Lett.* **10**, 710–717 (2007).
11. Tylianakis, J. M., Didham, R. K., Bascompte, J. & Wardle, D. A. Global change and species interactions in terrestrial ecosystems. *Ecol. Lett.* **11**, 1351–1363 (2008).
12. Dalsgaard, B. et al. Specialization in plant–hummingbird networks is associated with species richness, contemporary precipitation and Quaternary climate-change velocity. *PLoS ONE* **6**, e25891 (2011).
13. Dalsgaard, B. et al. Historical climate-change influences modularity and nestedness of pollination networks. *Ecography* **36**, 1331–1340 (2013).
14. Memmott, J., Waser, N. M. & Price, M. V. Tolerance of pollination networks to species extinctions. *Proc. R. Soc. Lond. B* **271**, 2605–2611 (2004).
15. Kaiser-Bunbury, C. N., Muff, S., Memmott, J., Müller, C. B. & Caflisch, A. The robustness of pollination networks to the loss of species and interactions: a quantitative approach incorporating pollinator behaviour. *Ecol. Lett.* **13**, 442–452 (2010).
16. Dáttilo, W. et al. Unravelling Darwin's entangled bank: architecture and robustness of mutualistic networks with multiple interaction types. *Proc. R. Soc. B* **283**, 20161564 (2016).
17. Dalsgaard, B. et al. Trait evolution, resource specialization and vulnerability to plant extinctions among Antillean hummingbirds. *Proc. R. Soc. B* **285**, 20172754 (2018).
18. Gilman, S. E., Urban, M. C., Tewksbury, J., Gilchrist, G. W. & Holt, R. D. A framework for community interactions under climate change. *Trends Ecol. Evol.* **25**, 325–331 (2010).
19. Rahbek, C. & Graves, G. R. Multiscale assessment of patterns of avian species richness. *Proc. Natl Acad. Sci. USA* **98**, 4534–4539 (2001).
20. Rahbek, C. & Graves, G. R. Detection of macro-ecological patterns in South American hummingbirds is affected by spatial scale. *Proc. R. Soc. Lond. B* **267**, 2259–2265 (2000).
21. Dalsgaard, B. et al. The influence of biogeographical and evolutionary histories on morphological trait-matching and resource specialization in mutualistic hummingbird–plant networks. *Funct. Ecol.* **35**, 1120–1133 (2021).
22. Sandel, B. et al. The influence of Late Quaternary climate-change velocity on species endemism. *Science* **334**, 660–664 (2011).
23. Scherrer, D. & Körner, C. Topographically controlled thermal-habitat differentiation buffers alpine plant diversity against climate warming. *J. Biogeogr.* **38**, 406–416 (2011).
24. Graves, G. R. & Rahbek, C. Source pool geometry and the assembly of continental avifaunas. *Proc. Natl Acad. Sci. USA* **102**, 7871–7876 (2005).
25. IPCC *Climate Change 2014: Impacts, Adaptation, and Vulnerability. Part B: Regional Aspects* (eds Barros, V. R. et al.) (Cambridge Univ. Press, 2014).
26. Hoegh-Guldberg, O. et al. in *Special Report on Global Warming of 1.5 °C* (eds Masson-Delmotte, V. et al.) 175–311 (IPCC, WMO, 2018).
27. Watson, J. E. M., Iwamura, T. & Butt, N. Mapping vulnerability and conservation adaptation strategies under climate change. *Nat. Clim. Change* **3**, 989–994 (2013).
28. Martín González, A. M., Dalsgaard, B. & Olesen, J. M. Centrality measures and the importance of generalist species in pollination networks. *Ecol. Complex.* **7**, 36–43 (2010).
29. Burgos, E. et al. Why nestedness in mutualistic networks? *J. Theor. Biol.* **249**, 307–313 (2007).
30. Bersier, L.-F., Banašek-Richter, C. & Cattin, M.-F. Quantitative descriptors of food-web matrices. *Ecology* **83**, 2394–2407 (2002).

31. Thébault, E. & Fontaine, C. Stability of ecological communities and the architecture of mutualistic and trophic networks. *Science* **329**, 853–856 (2010).
32. Tylianakis, J. M., Laliberté, E., Nielsen, A. & Bascompte, J. Conservation of species interaction networks. *Biol. Conserv.* **143**, 2270–2279 (2010).
33. Grass, I., Jauker, B., Steffan-Dewenter, I., Tscharntke, T. & Jauker, F. Past and potential future effects of habitat fragmentation on structure and stability of plant–pollinator and host–parasitoid networks. *Nat. Ecol. Evol.* **2**, 1408–1417 (2018).
34. Stouffer, D. B. & Bascompte, J. Compartmentalization increases food-web persistence. *Proc. Natl Acad. Sci. USA* **108**, 3648–3652 (2011).
35. Blüthgen, N., Menzel, F. & Blüthgen, N. Measuring specialization in species interaction networks. *BMC Ecol.* **6**, 9 (2006).
36. Dormann, C. F. & Strauss, R. A method for detecting modules in quantitative bipartite networks. *Methods Ecol. Evol.* **5**, 90–98 (2014).
37. Bascompte, J., Jordano, P., Melián, C. J. & Olesen, J. M. The nested assembly of plant–animal mutualistic networks. *Proc. Natl Acad. Sci. USA* **100**, 9383–9387 (2003).
38. Rahbek, C. et al. Humboldt's enigma: what causes global patterns of mountain biodiversity? *Science* **365**, 1108–1113 (2019).
39. Cracraft, J. Historical biogeography and patterns of differentiation within the South American avifauna: areas of endemism. *Ornithol. Monogr.* **36**, 49–84 (1985).
40. Hazzi, N. A., Moreno, J. S., Ortiz-Movliav, C. & Palacio, R. D. Biogeographic regions and events of isolation and diversification of the endemic biota of the tropical Andes. *Proc. Natl Acad. Sci. USA* **115**, 7985–7990 (2018).
41. Jønsson, K. A. et al. Tracking animal dispersal: from individual movement to community assembly and global range dynamics. *Trends Ecol. Evol.* **31**, 204–214 (2016).
42. McGuire, J. A. et al. Molecular phylogenetics and the diversification of hummingbirds. *Curr. Biol.* **24**, 910–916 (2014).
43. Proctor, M., Yeo, P. & Lack, A. *The Natural History of Pollination* (HarperCollins, 1996).
44. Simberloff, D. S. & Wilson, E. O. Experimental zoogeography of islands: the colonization of empty islands. *Ecology* **50**, 278–296 (1969).
45. Connor, E. F. & Simberloff, D. Species number and compositional similarity of the Galapagos flora and avifauna. *Ecol. Monogr.* **48**, 219–248 (1978).
46. Grant, P. R. & Abbott, I. Interspecific competition, island biogeography and null hypotheses. *Evolution* **34**, 332–341 (1980).
47. Thomas, C. D. Climate, climate change and range boundaries. *Divers. Distrib.* **16**, 488–495 (2010).
48. Almeida-Neto, M., Guimarães, P., Guimarães, P. R. Jr, Loyola, R. D. & Ulrich, W. A consistent metric for nestedness analysis in ecological systems: reconciling concept and measurement. *Oikos* **117**, 1227–1239 (2008).
49. Simmons, B. I. et al. Moving from frugivory to seed dispersal: incorporating the functional outcomes of interactions in plant–frugivore networks. *J. Anim. Ecol.* **87**, 995–1007 (2018).
50. Benadi, G., Blüthgen, N., Hovestadt, T. & Poethke, H.-J. Contrasting specialization–stability relationships in plant–animal mutualistic systems. *Ecol. Model.* **258**, 65–73 (2013).
51. Beckett, S. J. Improved community detection in weighted bipartite networks. *R. Soc. Open Sci.* **3**, 140536 (2016).
52. Sonne, J. et al. Ecological mechanisms explaining interactions within plant–hummingbird networks: morphological matching increases towards lower latitudes. *Proc. R. Soc. B* **287**, 20192873 (2020).
53. Patefield, W. Algorithm AS 159: an efficient method of generating random R×C tables with given row and column totals. *J. R. Stat. Soc. C* **30**, 91–97 (1981).
54. Dalsgaard, B. et al. Opposed latitudinal patterns of network-derived and dietary specialization in avian plant–frugivore interaction systems. *Ecography* **40**, 1395–1401 (2017).
55. Dormann, C. F., Gruber, B. & Fründ, J. Introducing the bipartite package: analysing ecological networks. *R News* **8**, 8–11 (2008).
56. Holt, B. G. et al. An update of Wallace's zoogeographic regions of the world. *Science* **339**, 74–78 (2013).
57. *Two-Minute Gridded Global Relief Data (ETOPO2)* v. 2 (NOAA National Geophysical Data Center, 2006); https://doi.org/10.7289/V5J1012Q
58. Jetz, W. & Rahbek, C. Geographic range size and determinants of avian species richness. *Science* **297**, 1548–1551 (2002).
59. Dobzhansky, T. Evolution in the tropics. *Am. Sci.* **38**, 209–221 (1950).
60. Currie, D. J., Francis, A. P. & Kerr, J. T. Some general propositions about the study of spatial patterns of species richness. *Écoscience* **6**, 392–399 (1999).
61. Hurlbert et al. The effect of energy and seasonality on avian species richness and community composition. *Am. Nat.* **161**, 83–97 (2003).
62. Karger, D. N. et al. Climatologies at high resolution for the Earth's land surface areas. *Sci. Data* **4**, 170122 (2017).
63. Mateo, R. G., Felicísimo, Á. M. & Muñoz, J. Effects of the number of presences on reliability and stability of MARS species distribution models: the importance of regional niche variation and ecological heterogeneity. *J. Veg. Sci.* **21**, 908–922 (2010).
64. Blonder, B. et al. Linking environmental filtering and disequilibrium to biogeography with a community climate framework. *Ecology* **96**, 972–985 (2015).
65. Vizentin-Bugoni, J., Debastiani, V. J., Bastazini, V. A. G., Maruyama, P. K. & Sperry, J. H. Including rewiring in the estimation of the robustness of mutualistic networks. *Methods Ecol. Evol.* **11**, 106–116 (2020).
66. Rahbek, C., Borregaard, M. K., Hermansen, B., Nogues-Bravo, D. & Fjeldså, J. *Definition and Description of the Montane Regions of the World* (Center for Macroecology, Evolution and Climate, 2019); https://macroecology.ku.dk/resources/mountain_regions/definition-and-description-of-the-montane-regions-of-the-world_kopi/
67. Hothorn, T., Bretz, F. & Westfall, P. Simultaneous inference in general parametric models. *Biom. J.* **50**, 346–363 (2008).

Acknowledgements

J.S. and C.R acknowledge the support of the VILLUM FONDEN for the Center for Global Mountain Biodiversity (grant no. 25925). A.M.M.G., C.R. and B.D. thank the Danish National Research Foundation for its support of the Center for Macroecology, Evolution, and Climate (grant no. DNRF96). P.K.M. thanks the support from Fapesp—The São Paulo Research Foundation (grant no. 2015/21457-4) and Fapemig—Minas Gerais Research Foundation (grant no. RED-00253-16). A.M.M.G. was supported through a Marie Skłodowska-Curie Individual Fellowship (H2020-MSCA-IF-2015-704409). J.B.'s work is supported by the Swiss National Science Foundation (grant no. 310030_197201).

Author contributions

J.S., C.R., J.B. and B.D. conceived the study. J.S. (with help from C.R. and J.B.) simulated and analysed the data. J.S. drafted the manuscript with input from P.K.M, A.M.M.G., C.R., J.B. and B.D. All authors contributed to the manuscript and gave final approval for its publication.

Competing interests

The authors declare no competing interests.

Additional information

Extended data is available for this paper at https://doi.org/10.1038/s41559-022-01693-3.

Supplementary information The online version contains supplementary material available at https://doi.org/10.1038/s41559-022-01693-3.

Correspondence and requests for materials should be addressed to Jesper Sonne.

Peer review information *Nature Ecology & Evolution* thanks Ricardo Dobrovolski and the other, anonymous, reviewer(s) for their contribution to the peer review of this work.

Reprints and permissions information is available at www.nature.com/reprints.

Publisher's note Springer Nature remains neutral with regard to jurisdictional claims in published maps and institutional affiliations.

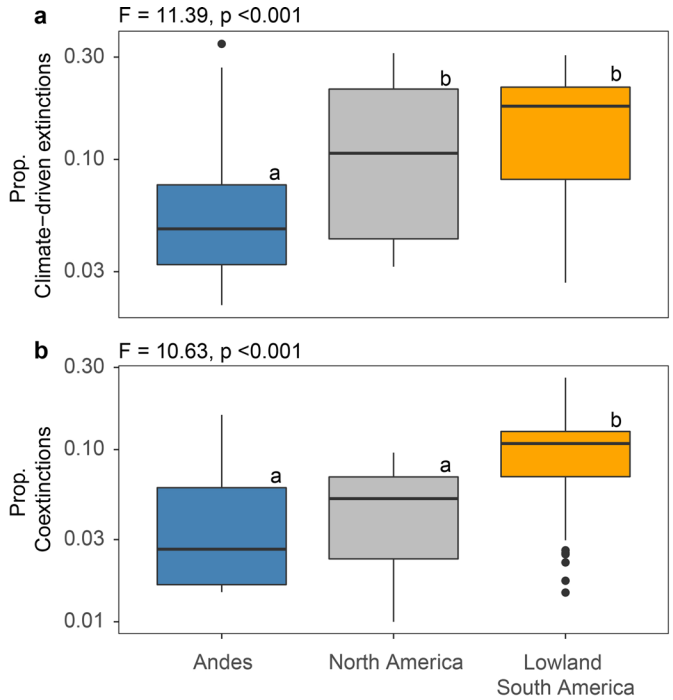

Extended Data Fig. 1 | Regional variability in climate-driven extinction (a) and coextinction (b) under the RCP 8.5 'worst case' scenario. Both extinction variables were scaled on logarithmic axes. We applied one-way ANOVA to test for regional differences in climate-driven extinctions and coextinctions (Climate-driven extinction: $F = 11.39$, $p < 0.001$, $n = 84$; Coextinction: $F = 10.63$, $p < 0.001$, $n = 84$). Lower case letters represent the statistical difference according to Tukey multiple comparisons with Bonferroni adjusted p values ($p < 0.05$). The boxes' border marks the interquartile range (IQR; quartile 1 to 3); horizontal lines inside boxes mark the medians; vertical lines mark $\pm 1.5 \times$ (IQR); the circles mark data outliers. The results depicted here derive from the RCP 8.5 "worst case" scenario for the year 2070.

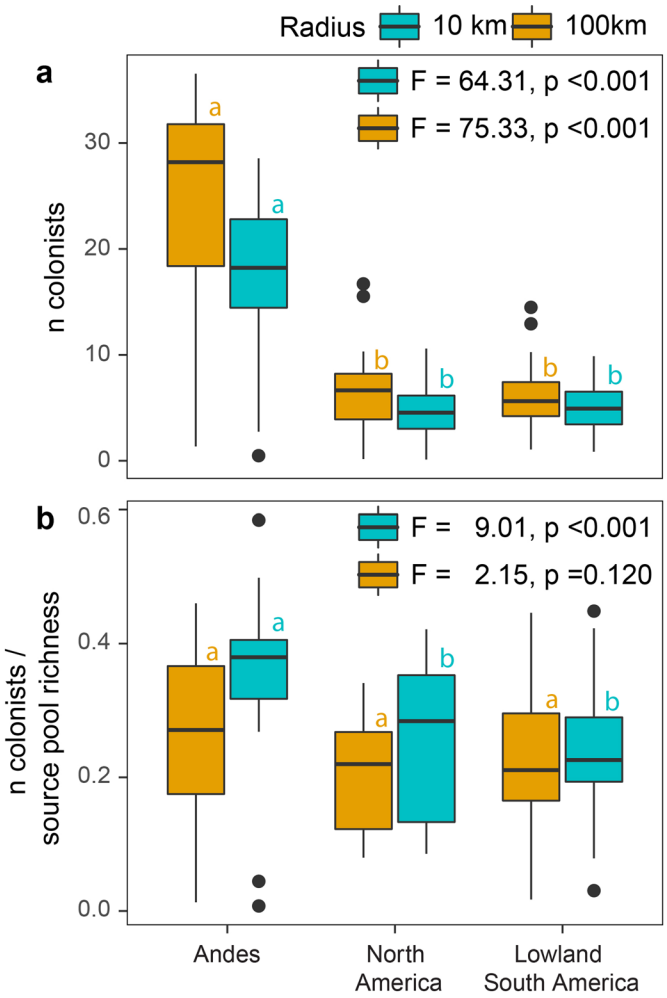

Extended Data Fig. 2 | Biogeographical variability in colonization rates under the RCP 8.5 'worst case' scenario. Colonization rates are measured as the average number of colonizing from a radius of 10 km ($F = 64.31$, $p < 0.001$, $n = 84$) and 100 km ($F = 75.33$, $p < 0.001$, $n = 84$) surrounding each network (a). Panel b depicts the number of colonists relative to the richness of hummingbirds within the source pool radius (10 km radius: $F = 9.01$, $p < 0.001$, $n = 84$; 10 km radius: $F = 2.15$, $p = 0.120$, $n = 84$). We applied one-way ANOVA to test for differences in colonization rate between biogeographical regions. The boxes' border marks the interquartile range (IQR; quartile 1 to 3); horizontal lines inside boxes mark the medians; vertical lines mark ±1.5 × (IQR); the circles mark data outliers. Lower-case letters represent statistical difference according to Tukey multiple comparisons with Bonferroni-adjusted p values ($p < 0.05$). The results depicted derive from the RCP 8.5 'worst case' scenario for the year 2070.

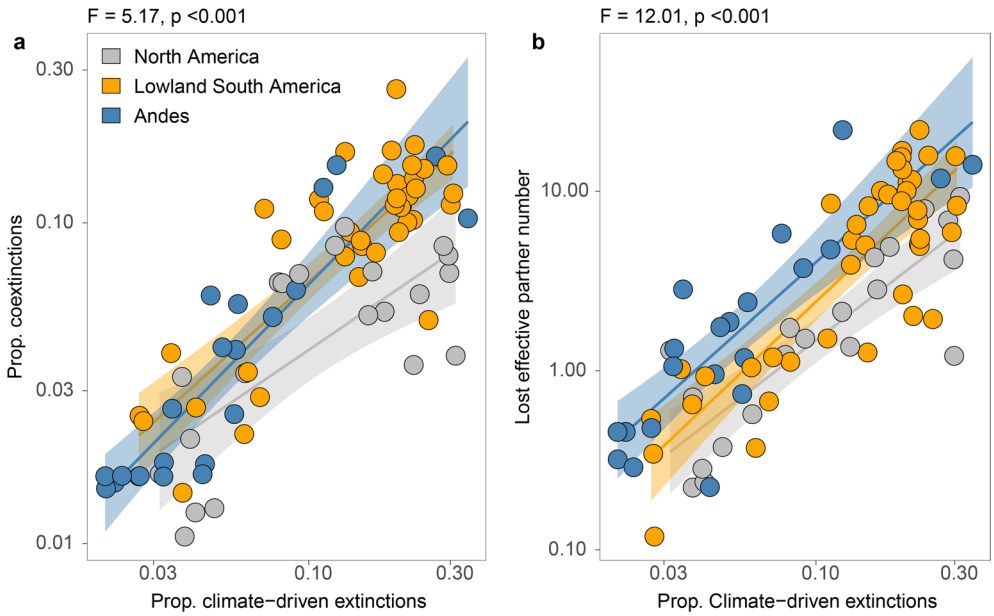

Extended Data Fig. 3 | Biogeographical variability in the communities' vulnerability to coextinctions after accounting for climate-driven extinctions under the RCP 8.5 'worst case' scenario. Coextinctions spread slower in North America compared to other regions (a, $F = 5.17$, $p < 0.001$, $n = 83$), which coincide with a regional bias in climate-driven extinctions against species with generalized network roles (b, $F = 12.01$, $p < 0.001$, $n = 83$). The species-level generalism was described by the *effective number of partners*. The F-test in each panel compares two linear regression models, of which one contains the biogeographical region as a character state predictor variable. The solid lines represent the linear relationships within each region (with shaded 95% confidence intervals). The y axes measure the cumulative lost partner number averaged across the simulations. The results depicted here derive from the RCP 8.5 'worst case' scenario for the year 2070.

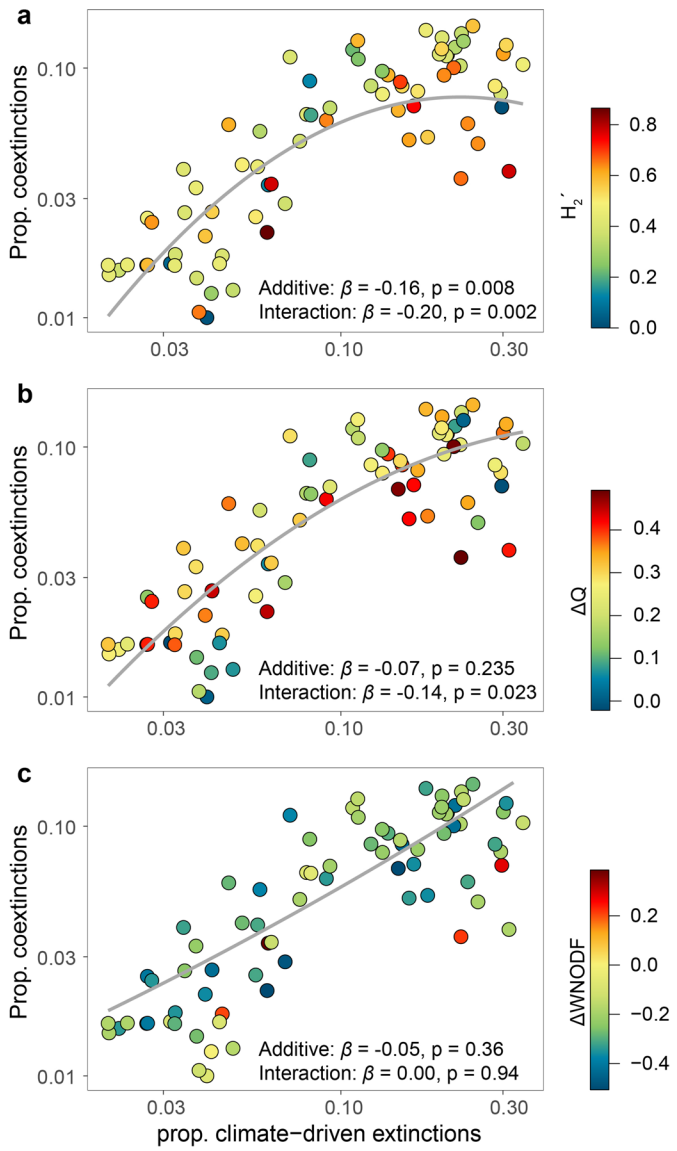

Extended Data Fig. 4 | The influence of three network structures on the logarithmic association between climate-driven extinctions and coextinctions (n = 83) under the RCP 8.5 'worst case' scenario. The three network structures are Complementary specialization (H2'), Modularity (ΔQ) and nestedness (ΔWNODF). Trend lines and standardized coefficients derive from weighted multiple linear regressions. In each regression model, we added an interaction term between the proportion of climate-driven extinctions and the network metric. The weights were given by the number of hummingbird species sampled in each network. The results derive from the RCP 8.5 'worst case' scenario for the year 2070.

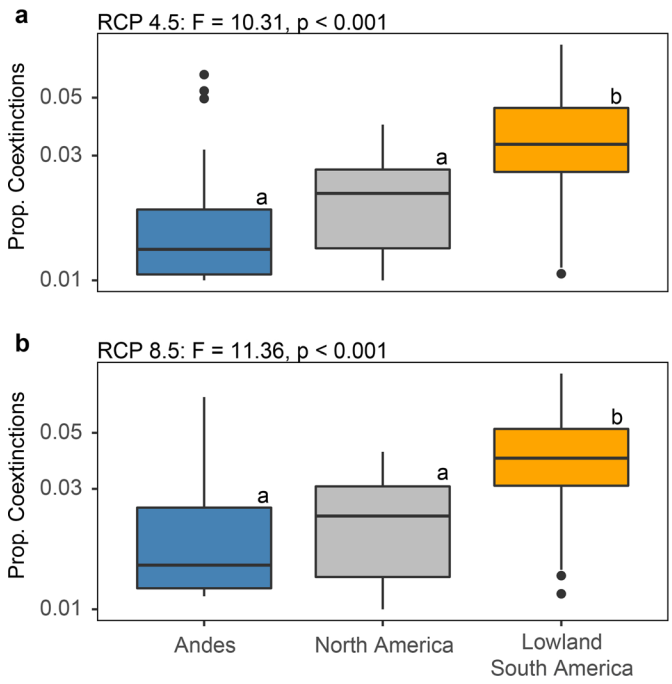

Extended Data Fig. 5 | Geographical variation in coextinctions, measured as the average proportion of hummingbirds in our simulations that disappeared from the networks while accounting for interaction rewiring. In this analysis, we allowed species to relocate 50 % of their lost interactions with remaining partners in the network (that is constrained rewiring). The F-statistics derive from one-way ANOVA testing for regional differences in coextinctions (RCP 4.5: $F = 10.31$, $p < 0.001$, $n = 84$; RCP 8.5: $F = 11.36$, $p < 0.001$, $n = 84$; note the logarithmic axes). Lower-case letters represent the statistical difference according to Tukey multiple comparisons with Bonferroni-adjusted p values s ($p < 0.05$). The boxes' border marks the interquartile range (IQR; quartile 1 to 3); horizontal lines inside boxes mark the medians; vertical lines mark $\pm 1.5 \times$ (IQR); the circles mark data outliers. The results are replicated for the RCP 4.5 'mid-range' scenario (a) and the RCP 8.5 'worst case" scenario for the year 2070 (b).

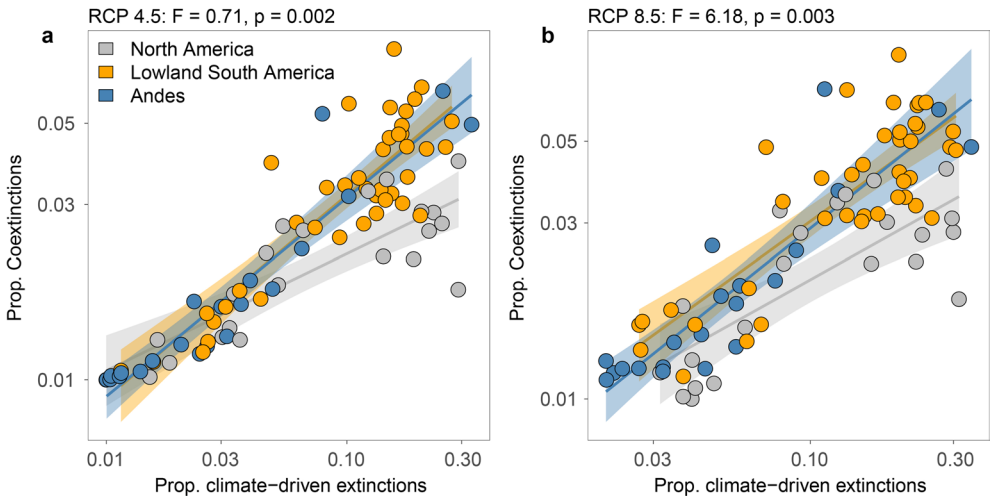

Extended Data Fig. 6 | Biogeographical variability in the communities' vulnerability to coextinctions after accounting for climate-driven extinctions and interaction rewiring. The analyses are similar to those depicted in Fig. 4a, although, here, we allowed species to relocate 50 % of their lost interactions with remaining partners in the network (that is constrained rewiring). The F-test in each panel compares two linear regression models, of which one contains the biogeographical region as a character state predictor variable. The solid lines represent the linear relationships within each region (with shaded 95% confidence intervals). The results are replicated for the RCP 4.5 'mid-range' scenario (a) and the RCP 8.5 'worst case' scenario for the year 2070 (b).

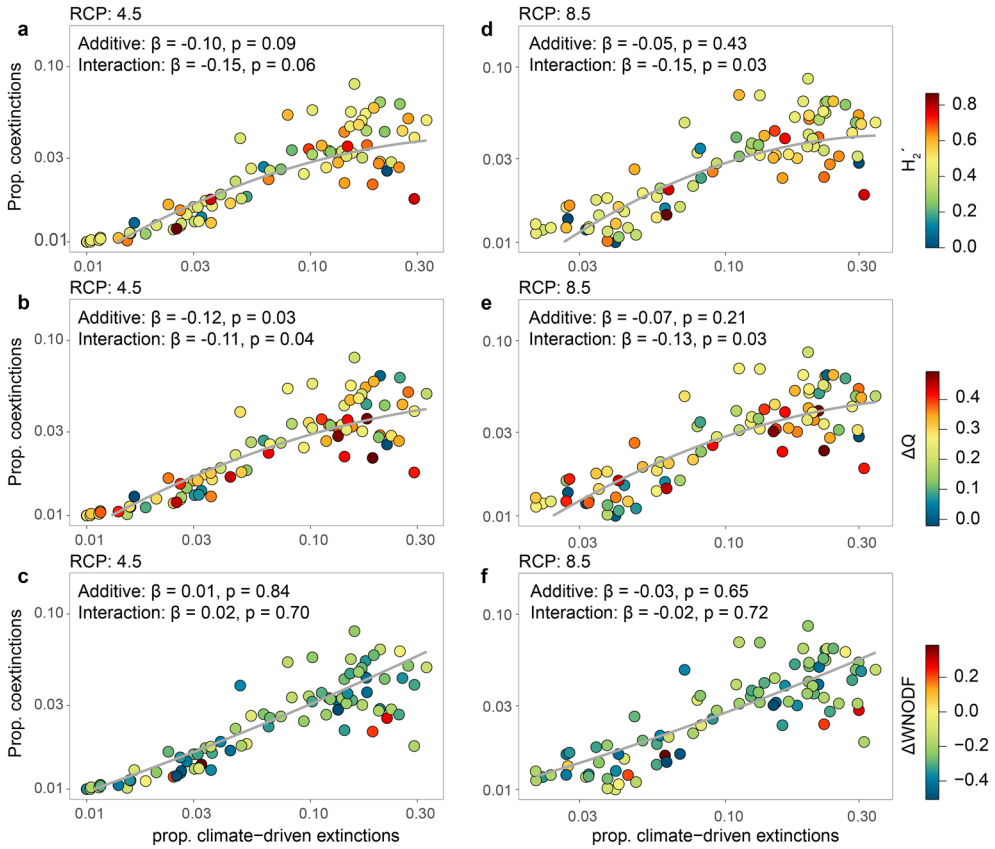

Extended Data Fig. 7 | The influence of three network structures on the logarithmic association between climate-driven extinctions and coextinctions (n = 83) while accounting for interaction rewiring. Here, we allowed species to relocate 50% of their lost interactions with remaining partners in the network (i.e. constrained rewiring). The three network structures are Complementary specialization (H_2'), Modularity (ΔQ) and nestedness (ΔWNODF). Trend lines and standardized coefficients derive from weighted multiple linear regressions. In each regression model, we added an interaction term between the proportion of climate-driven extinctions and the network metric. The weights were given by the number of hummingbird species sampled in each network. The results are replicated for the RCP 4.5 'mid-range' scenario (a-c) and the RCP 8.5 'worst case' scenario for the year 2070 (d-f).

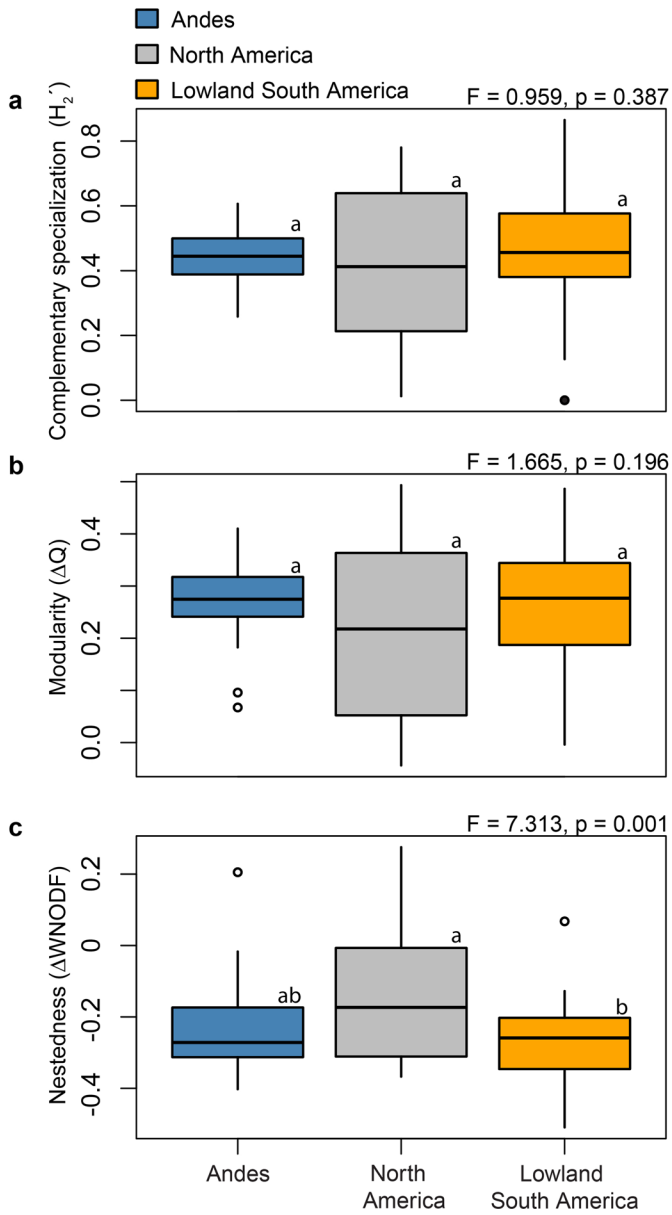

Extended Data Fig. 8 | Boxplots showing the regional variability in three network structures. Complementary specialization (a, F = 0.96, p = 0.387, n = 84), modularity (b, F = 1.67, p = 0.196, n = 84), and nestedness (c, F = 7.31, p = 0.001, n = 84). Δ signs indicate corrections by Patefield's null model 4. To test for variability in each network structure between the three biogeographical regions, we applied one-way ANOVA. The boxes' border marks the interquartile range (IQR; quartile 1 to 3); horizontal lines inside boxes mark the medians; vertical lines mark ±1.5 × (IQR); the circles mark data outliers. Lower case letters represent the statistical difference according to Tukey multiple comparisons with Bonferroni adjusted p values s ($p < 0.05$). Before calculations, we removed boreal hummingbird migrants from the networks to match our extinction simulations.

nature portfolio

Corresponding author(s): Jesper Sonne

Last updated by author(s): Jan 31, 2022

Reporting Summary

Nature Portfolio wishes to improve the reproducibility of the work that we publish. This form provides structure for consistency and transparency in reporting. For further information on Nature Portfolio policies, see our Editorial Policies and the Editorial Policy Checklist.

Statistics

For all statistical analyses, confirm that the following items are present in the figure legend, table legend, main text, or Methods section.

n/a	Confirmed	
☐	☒	The exact sample size (*n*) for each experimental group/condition, given as a discrete number and unit of measurement
☐	☒	A statement on whether measurements were taken from distinct samples or whether the same sample was measured repeatedly
☐	☒	The statistical test(s) used AND whether they are one- or two-sided *Only common tests should be described solely by name; describe more complex techniques in the Methods section.*
☐	☒	A description of all covariates tested
☐	☒	A description of any assumptions or corrections, such as tests of normality and adjustment for multiple comparisons
☐	☒	A full description of the statistical parameters including central tendency (e.g. means) or other basic estimates (e.g. regression coefficient) AND variation (e.g. standard deviation) or associated estimates of uncertainty (e.g. confidence intervals)
☐	☒	For null hypothesis testing, the test statistic (e.g. *F*, *t*, *r*) with confidence intervals, effect sizes, degrees of freedom and *P* value noted *Give P values as exact values whenever suitable.*
☒	☐	For Bayesian analysis, information on the choice of priors and Markov chain Monte Carlo settings
☒	☐	For hierarchical and complex designs, identification of the appropriate level for tests and full reporting of outcomes
☒	☐	Estimates of effect sizes (e.g. Cohen's *d*, Pearson's *r*), indicating how they were calculated

Our web collection on statistics for biologists contains articles on many of the points above.

Software and code

Policy information about availability of computer code

Data collection	We did not use software code in the data collection process
Data analysis	All analyses, simulations, and data handling were conducted in R version 4.0.3. Network structure and roles were analysed using the 'bipartite' R package v. 2.11. Multiple comparison analyses were conducted using the 'multcomp' R package. Algorithms used to conduct the analyses are provided at the Figshare Repository: https://doi.org/10.6084/m9.figshare.19071752.v2

For manuscripts utilizing custom algorithms or software that are central to the research but not yet described in published literature, software must be made available to editors and reviewers. We strongly encourage code deposition in a community repository (e.g. GitHub). See the Nature Portfolio guidelines for submitting code & software for further information.

Data

Policy information about availability of data

All manuscripts must include a data availability statement. This statement should provide the following information, where applicable:

- Accession codes, unique identifiers, or web links for publicly available datasets
- A description of any restrictions on data availability
- For clinical datasets or third party data, please ensure that the statement adheres to our policy

Data used to conduct the analysis are provided at the Figshare Repository: https://doi.org/10.6084/m9.figshare.19071752.v2

Field-specific reporting

Please select the one below that is the best fit for your research. If you are not sure, read the appropriate sections before making your selection.

☒ Life sciences ☐ Behavioural & social sciences ☐ Ecological, evolutionary & environmental sciences

For a reference copy of the document with all sections, see nature.com/documents/nr-reporting-summary-flat.pdf

Life sciences study design

All studies must disclose on these points even when the disclosure is negative.

Sample size	The sample dataset comprise all 84 mainland hummingbird-plant networks published in Dalsgaard et al. 2021. These comprise 169 hummingbird species and 1201 plant species on the mainland Americas. The complete sample dataset consists of networks from the Temperate North America to Southern Brazil. Hence, it is appropriate for large-scale analyses
Data exclusions	Compared to the published database, we excluded nine Caribbean island networks (11 hummingbird species and 55 plant species). On islands, area and isolation strongly influence species assembly, making the extinction-colonization dynamics non-analogous to the mainland. Moreover, island species usually have small ranges constrained by the sea rather than climate, which complicates climate niche modeling.
Replication	The processes of climate-driven extinction, coextinction and colonization were simulated 1000 times for two different climate scenarios: Representative Concentration Pathway (RCP) 4.5 “mid-range” scenario and RCP 8.5 “worst-case” scenario for the year 2070. Moreover, we replicated the coextinction simulations by allowing species to relocate 50% of their lost interactions with remaining partners in the network. This replication was done to test the assumption of strict mutual dependencies between species. Our results were robust to the variability between future climate scenarios and the species’ adaptability to mutualistic partner loss
Randomization	The processes of climate-driven extinction, coextinction and colonization were simulated as stochastic processes. We did not use experiamental groups. Hence, random allocation of groups is not relevant here
Blinding	This study is based on observational field studies of hummingbird-plant interactions collected over decades. This observational data type does not involve experimental treatments (which would be impossible given the scale of the analyses). Hence, blinding procedures were not applicable.

Reporting for specific materials, systems and methods

We require information from authors about some types of materials, experimental systems and methods used in many studies. Here, indicate whether each material, system or method listed is relevant to your study. If you are not sure if a list item applies to your research, read the appropriate section before selecting a response.

Materials & experimental systems

n/a	Involved in the study
☒	☐ Antibodies
☒	☐ Eukaryotic cell lines
☒	☐ Palaeontology and archaeology
☒	☐ Animals and other organisms
☒	☐ Human research participants
☒	☐ Clinical data
☒	☐ Dual use research of concern

Methods

n/a	Involved in the study
☒	☐ ChIP-seq
☒	☐ Flow cytometry
☒	☐ MRI-based neuroimaging